Simultaneous three-dimensional vascular and tubular imaging of whole mouse kidneys with X-ray µCT

Supplemental Information

Willy Kuo[a,b,c], Ngoc An Le[d], Bernhard Spingler[d], Roland H. Wenger[a,b], Anja Kipar[e], Udo Hetzel[f], Georg Schulz[c], Bert Müller[c,*], Vartan Kurtcuoglu[a,b,*]

[a.] Institute of Physiology, University of Zurich, Winterthurerstrasse 190, 8057 Zurich, Switzerland;

[b.] National Centre of Competence in Research, Kidney.CH, University of Zurich, Winterthurerstrasse 190, 8057 Zurich, Switzerland;

[c.] Biomaterials Science Center, Department of Biomedical Engineering, University of Basel, Gewerbestrasse 14, 4123 Allschwil, Switzerland

[d.] Department of Chemistry, University of Zurich, Winterthurerstrasse 190, 8057 Zurich, Switzerland;

[e.] Laboratory for Animal Model Pathology (LAMP), Institute of Veterinary Pathology, Vetsuisse Faculty, University of Zurich, Winterthurerstrasse 268, 8057 Zurich, Switzerland

[f.] Electron Microscopy Unit, Institute of Veterinary Pathology, Vetsuisse Faculty, University of Zurich, Winterthurerstrasse 268, 8057 Zurich, Switzerland

[g.] Zurich Center for Integrative Human Physiology, University of Zurich, Zurich, Switzerland

[*] These authors contributed equally

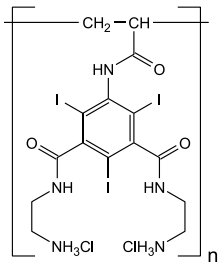**Corresponding author:**
Vartan Kurtcuoglu

University of Zürich
Institute of Physiology
Winterthurerstr. 190
8057 Zürich

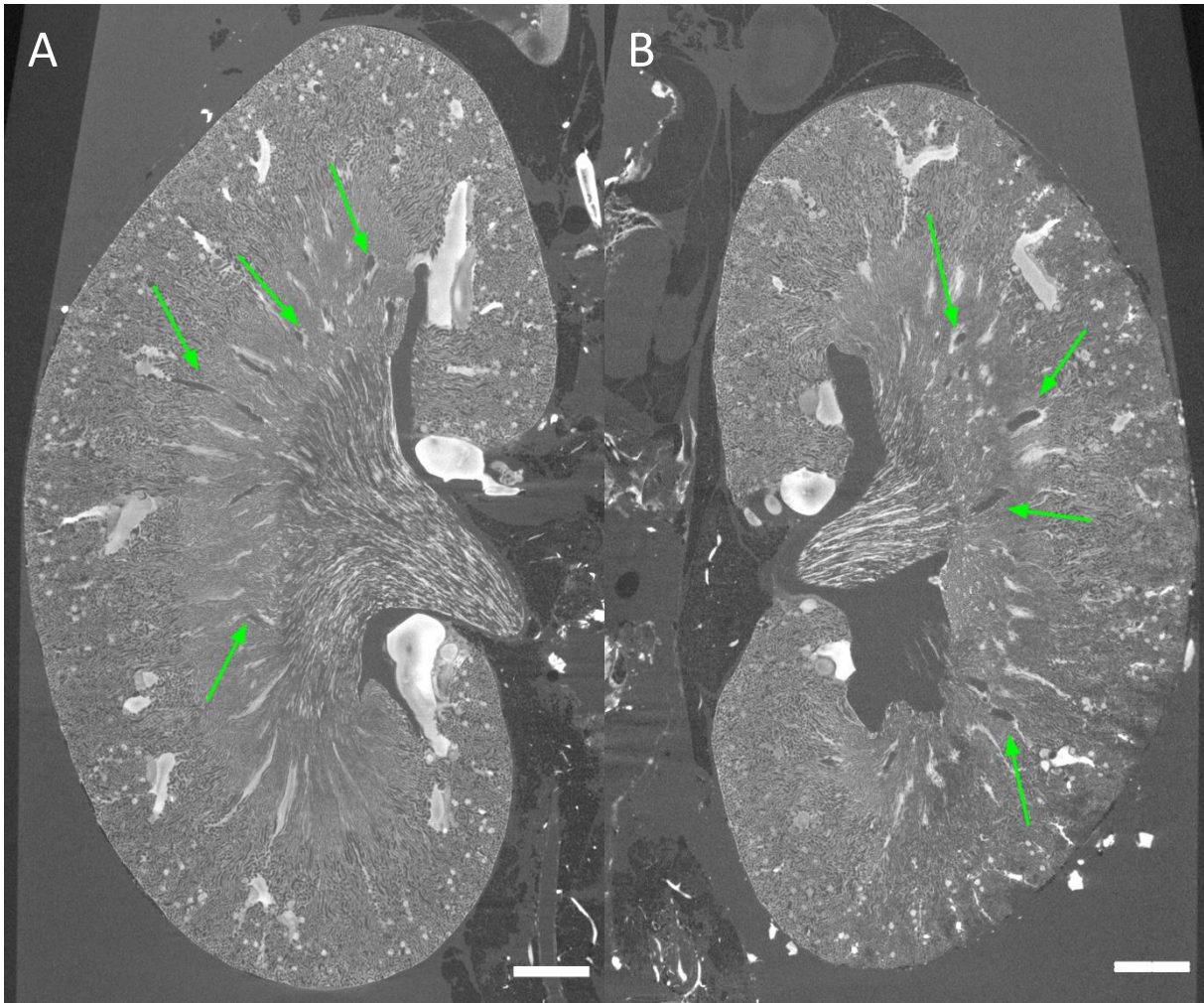Tel: +41 44 635 50 55
Fax: +41 44 635 68 14
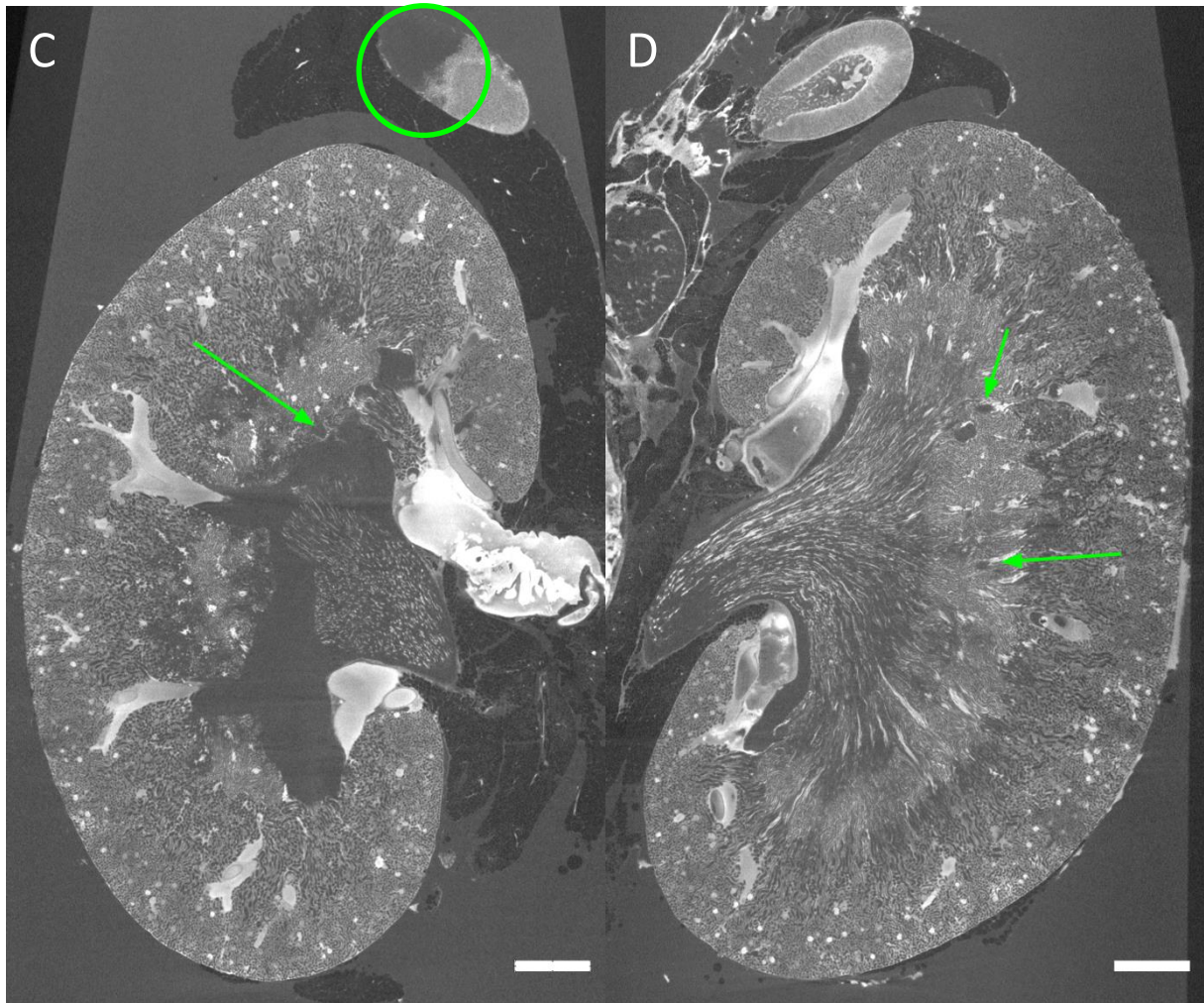E-mail: vartan.kurtcuoglu@uzh.ch

Supplemental Fig. S1: Polymeric X-ray contrast agent formula

Supplemental Fig. S1. Chemical formula of the polymeric X-ray contrast agent prior to pre-crosslinking with glutaraldehyde.

# Supplemental Fig. S2: Fluid-filled structures in kidneys of aged mice

Supplemental Fig. S2. *A*: Left kidney of a 10 month old female C57BL/6J mouse. A number of fluid-filled structures are indicated by green arrows. These structures cannot be captured by previous vascular casting protocols, and were identified as tubular protein casts based on the subsequent histological examination (Fig 2.). Voxel size 4.4 µm. Scale bar: 1 mm. *B*: Right kidney of the same mouse. *C*: Left kidney of a different 10 month old female C57BL/6J mouse. Fluid-filled structures are indicated by green arrows. Part of the left adrenal gland is unperfused, while the rest is completely perfused (green circle). This region is likely supplied by vessels other than the renal artery and were not perfused due to the ligations applied to the abdominal aorta and superior mesenteric artery. Voxel size 4.4 µm. Scale bar: 1 mm. *D*: Right kidney of the same mouse. The right adrenal gland is fully perfused.

**Supplemental Fig. S3: Transmission electron microscopy**
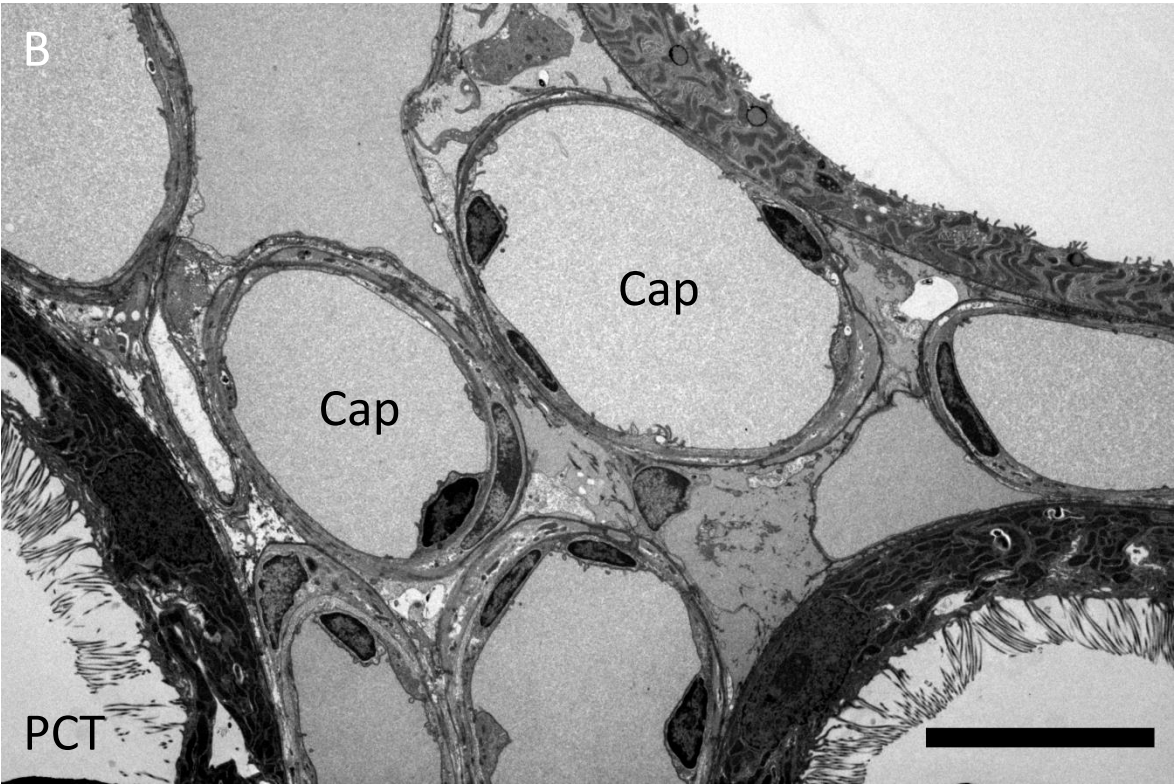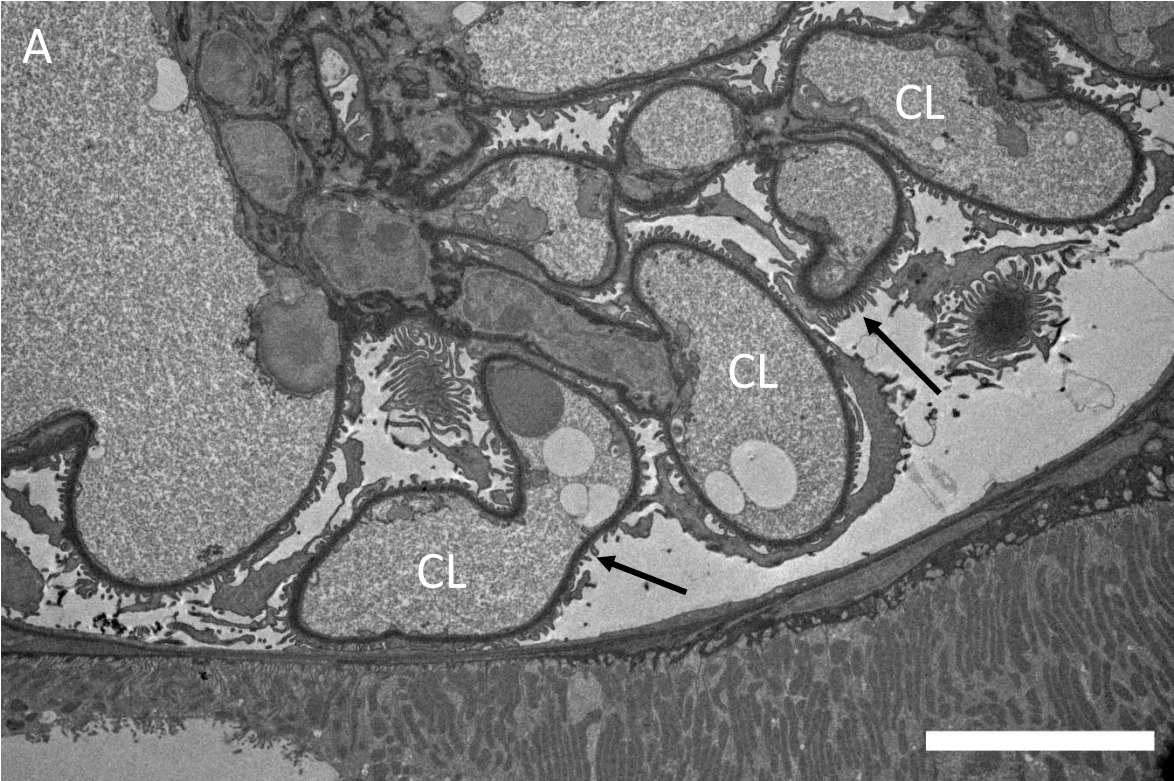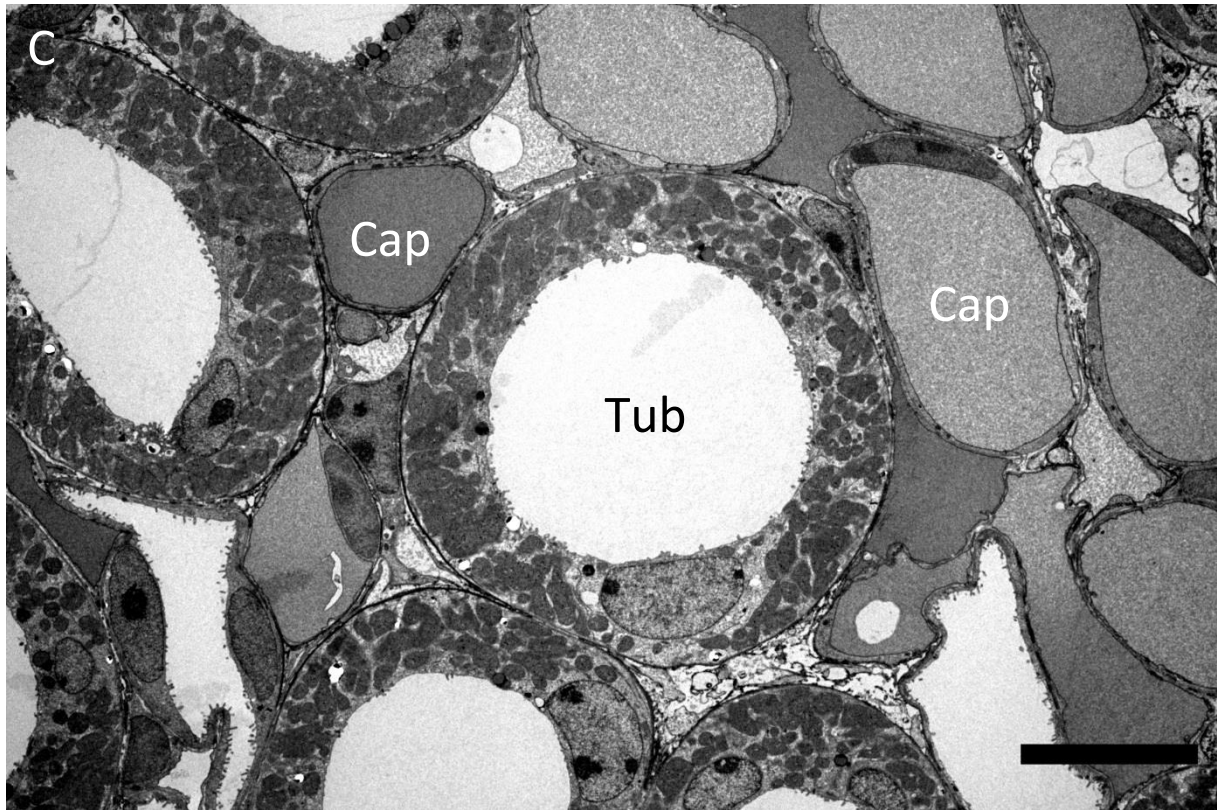
Supplemental Fig. S3. Transmission electron microscopy (TEM) images confirm that instillation of the contrast agent does not induce any tissue damage. *A*: Cortex. Non-contrasted TEM image of part of a glomerulus. Contrast agent is visible as coarsely granular material within the lumen of mesangial capillary loops (CL), and not found in the Bowman's space. Capillary loops are delineated by basement membrane with podocyte foot processes (arrows). Scale bar: 10 µm. *B*: Cortex. Contrasted TEM image of interstitial cortical capillaries (Cap) containing finely granular contrast agent. PCT - proximal convoluted tubule with intact ciliated epithelial cells. *C*: Medulla. Contrasted TEM image of interstitial cortical capillaries (Cap) containing moderately granular contrast agent of variable electron density. Tub - tubule with intact non-ciliated mitochondria rich epithelial cell. Scale bar: 10 µm.

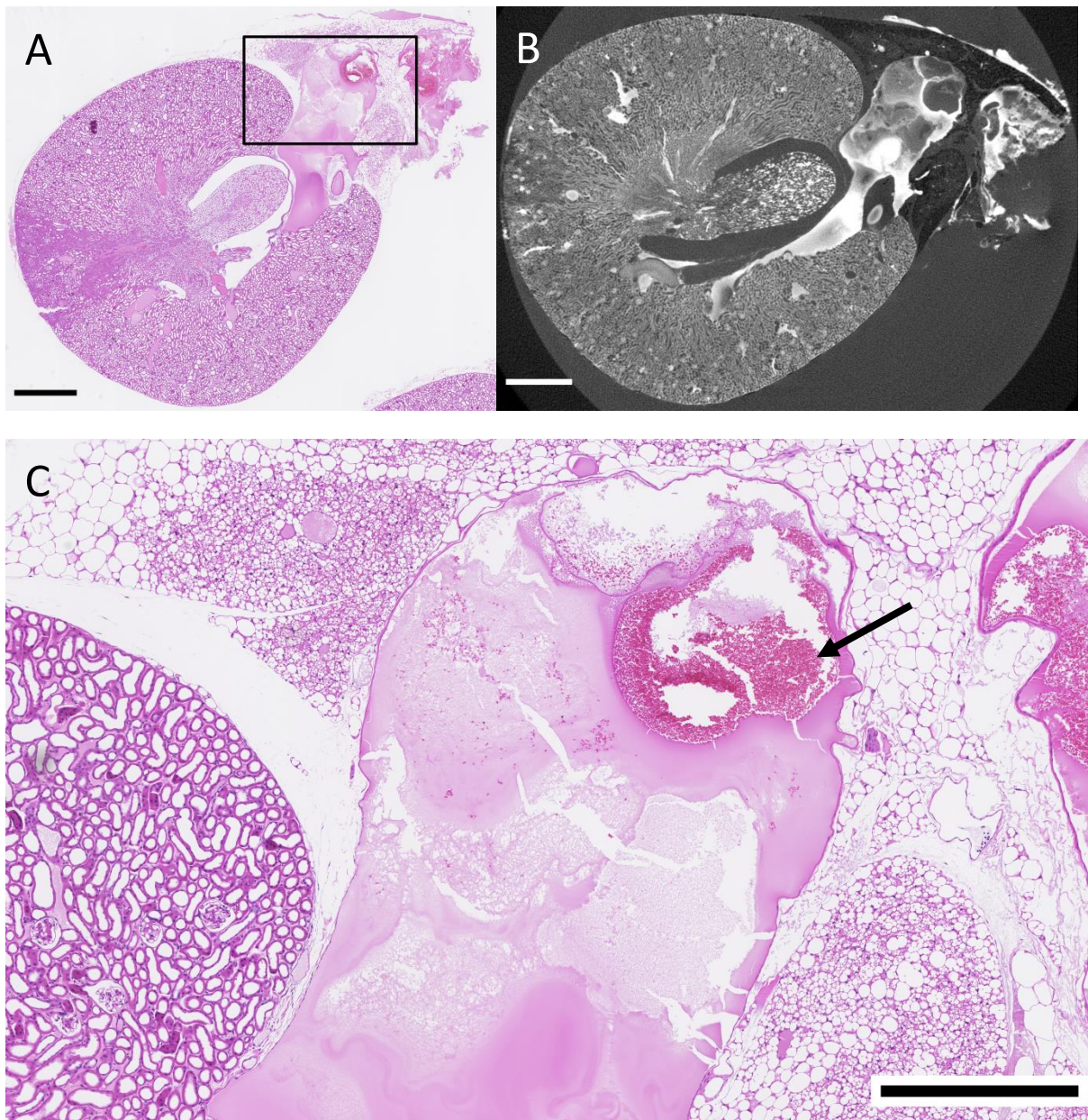# Supplemental Fig. S4: Histology of inadequately perfused kidney region
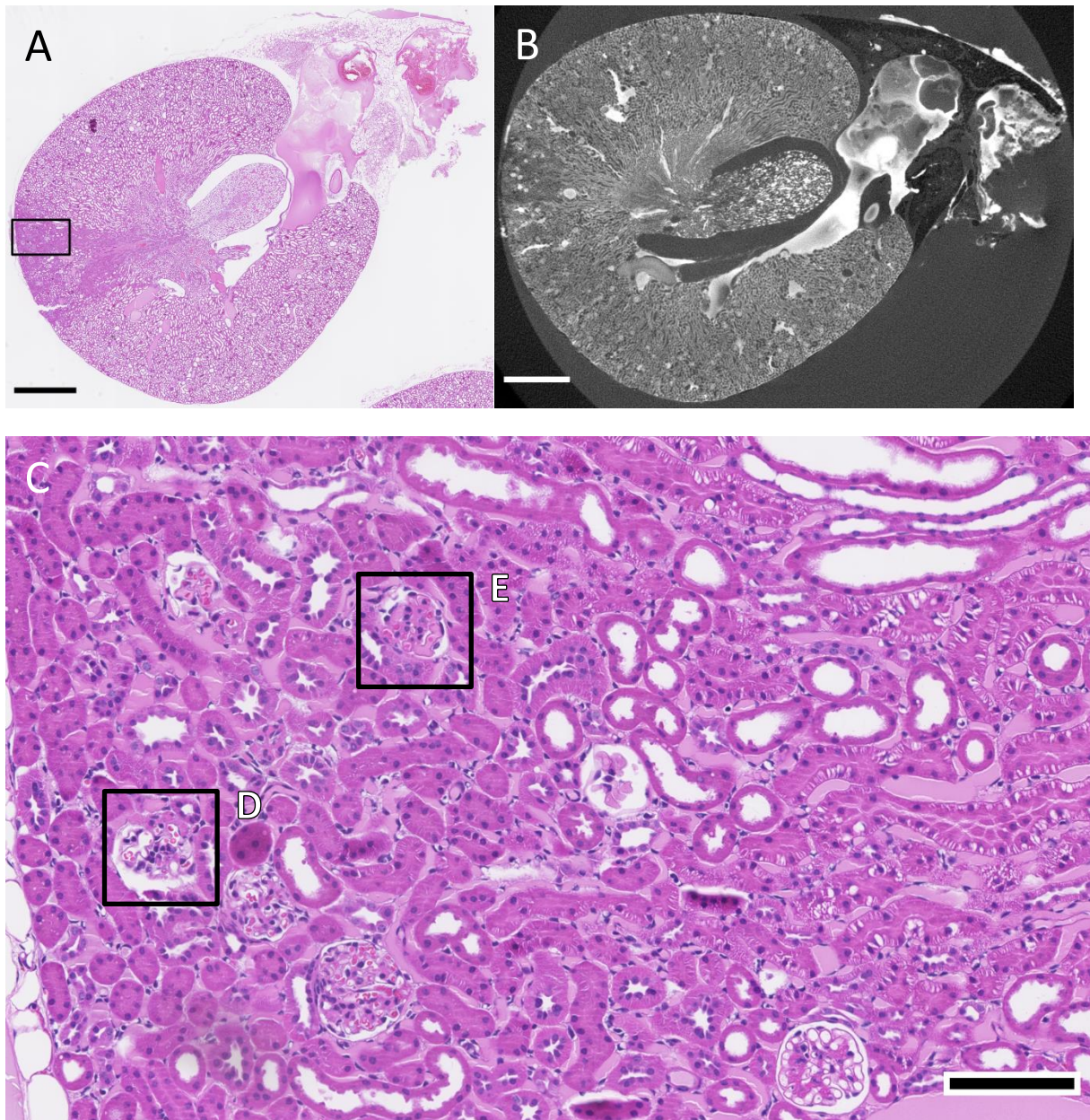
Supplemental Fig. S4. *A*: Overview image of an HE-stained histological section showing an inadequately perfused region. HE-stained slides and unstained slides for evaluation of fluorescence were scanned using a digital slide scanner (NanoZoomer-XR C12000; Hamamatsu, Hamamatsu City, Japan) with 40× magnification. Pixel size: Downsampled 8× to 1.8 µm. Scale bar: 1 mm. *B*: Similar virtual section from the X-ray µCT dataset. Pixel size: 4.4 µm. Scale bar: 1 mm *C*: Higher magnification of the improperly perfused region highlighted in A. Glomeruli show abundant red blood cells (D), indicating an insufficient initial flushing of the glomeruli as the cause of the collapsed tubuli. Contrast agent is visible in some of the glomeruli along with the red blood cells in both the histology and the X-ray µCT dataset (E), indicating filling of the vessels despite blockage via remaining red blood cells. Pixel size: 227 nm. Scale bar: 100 µm.
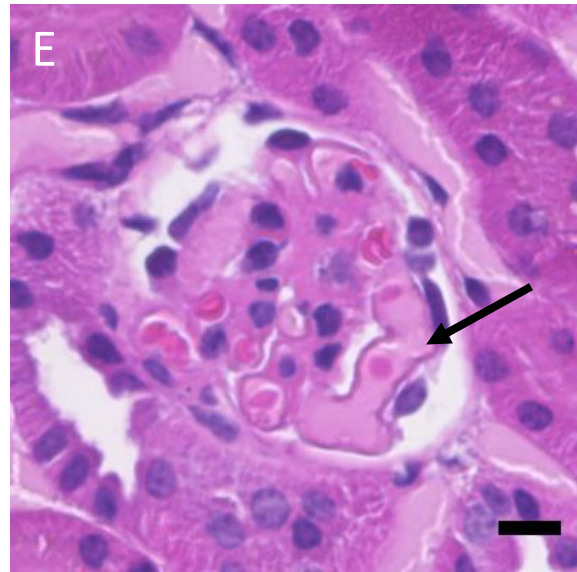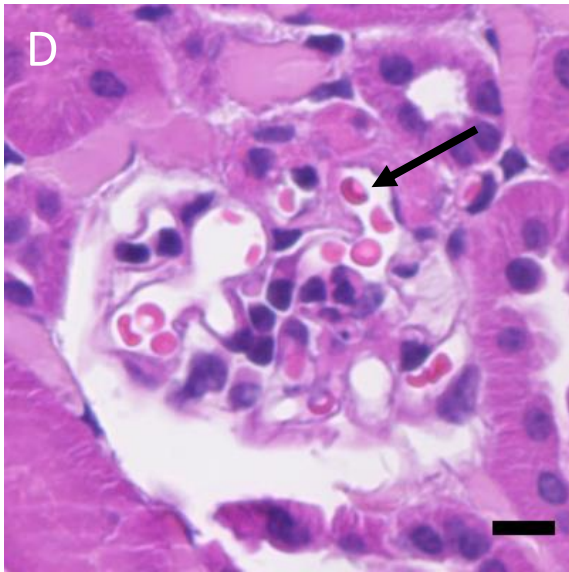
Supplemental Fig. S4. *D*: Higher magnification of a glomerulus showing abundant red blood cells highlighted in C. Scale bar: 10 µm. *E*: Higher magnification of a glomerulus filled with X-ray contrast agent and red blood cells highlighted in C.

Supplemental Fig. S5: Histology of low contrast region in renal vein

Supplemental Fig. S5. *A*: Overview image of an HE-stained histological section showing an improperly perfused region. Pixel size: Downsampled 8× to 1.8 µm. Scale bar: 1 mm. *B*: Similar virtual section from the X-ray µCT dataset. Pixel size: 4.4 µm. Scale bar: 1 mm *C*: Region of interest showing the renal vein. The low contrast regions seen in the X-ray µCT dataset are represented by a foam-like mixture of contrast agent with water or blood (aggregates of red blood cells (arrow) and/or fibrin), which may be caused by backflow of blood from the non-perfused parts of the remaining mouse body and resulting dilution of the contrast agent. Pixel size: Downsampled 2× to 454 nm. Scale bar: 500 µm.

Supplemental Fig. S6: Histogram and segmentation
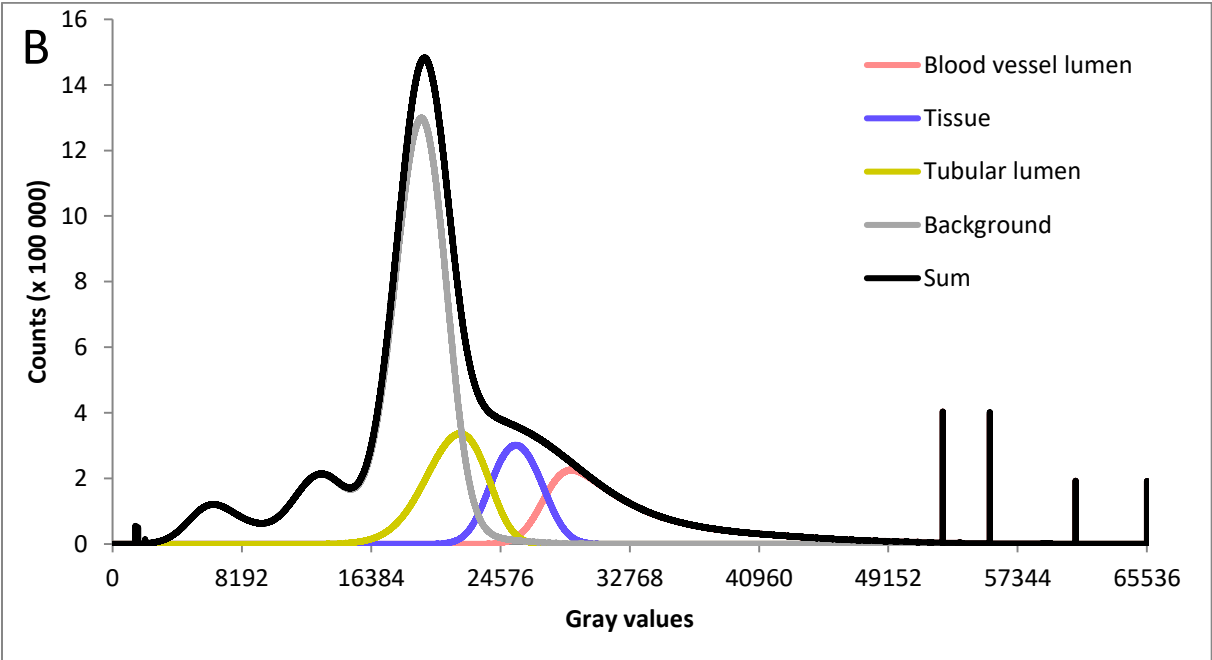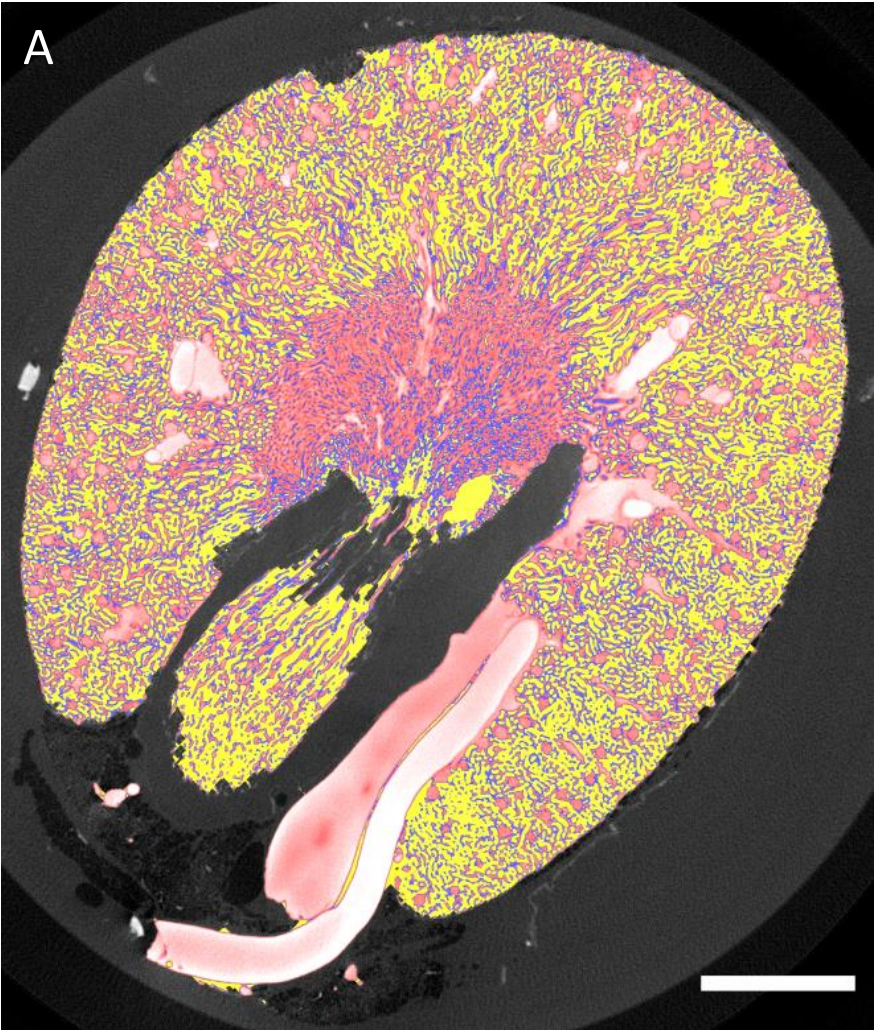
Supplemental Fig. S6. *A*: Overlay of segmentations of blood vessels (red), tissue (blue) and tubules over original raw data. Scale bar: 1 mm. *B*: Histogram of the whole dataset.

Supplemental Fig. S7: Line intensity profile
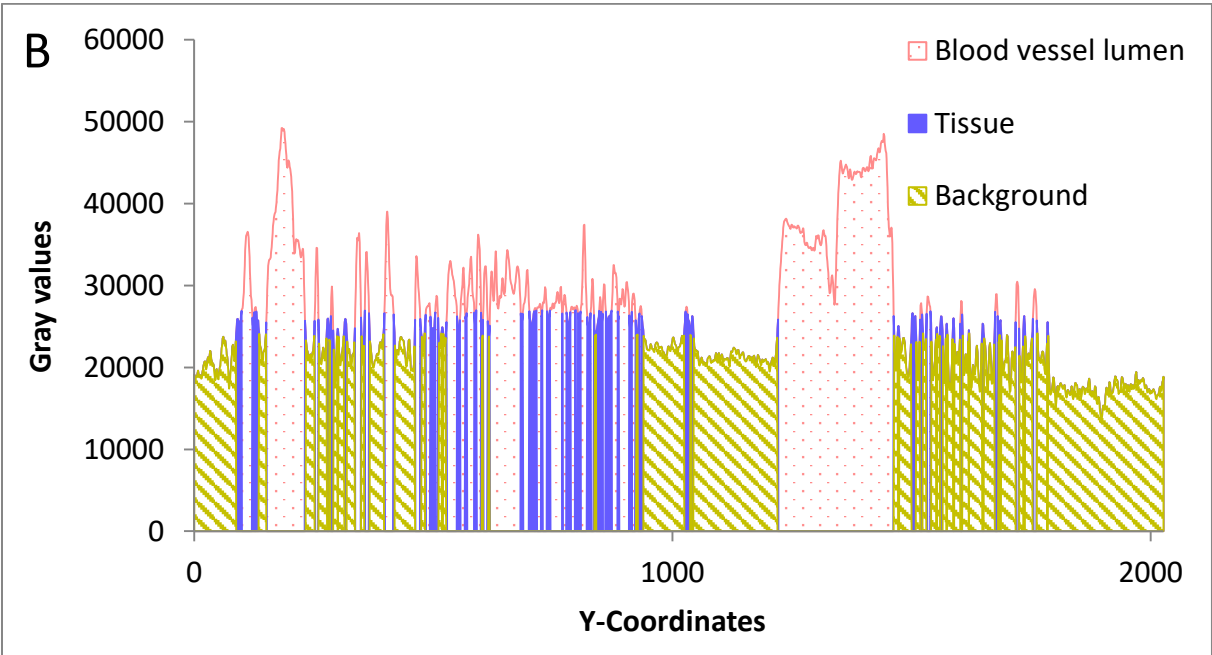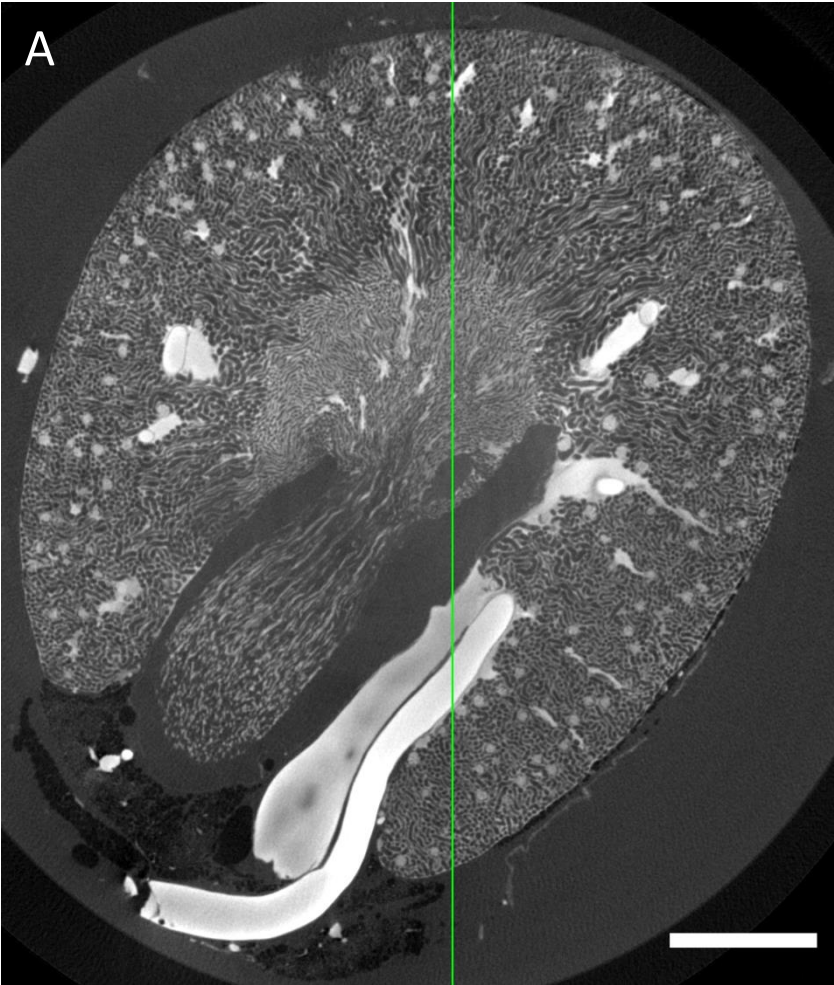
Supplemental Fig. S7. *A*: Single virtual section of the Gauss-filtered 3.3 µm voxel size dataset. The green line indicates line probe location. Scale bar: 1 mm. *B*: Profile along the line probe colored according to the thresholds used for segmentation.

Supplemental Fig. S8: UV-Vis spectrum of the contrast agent
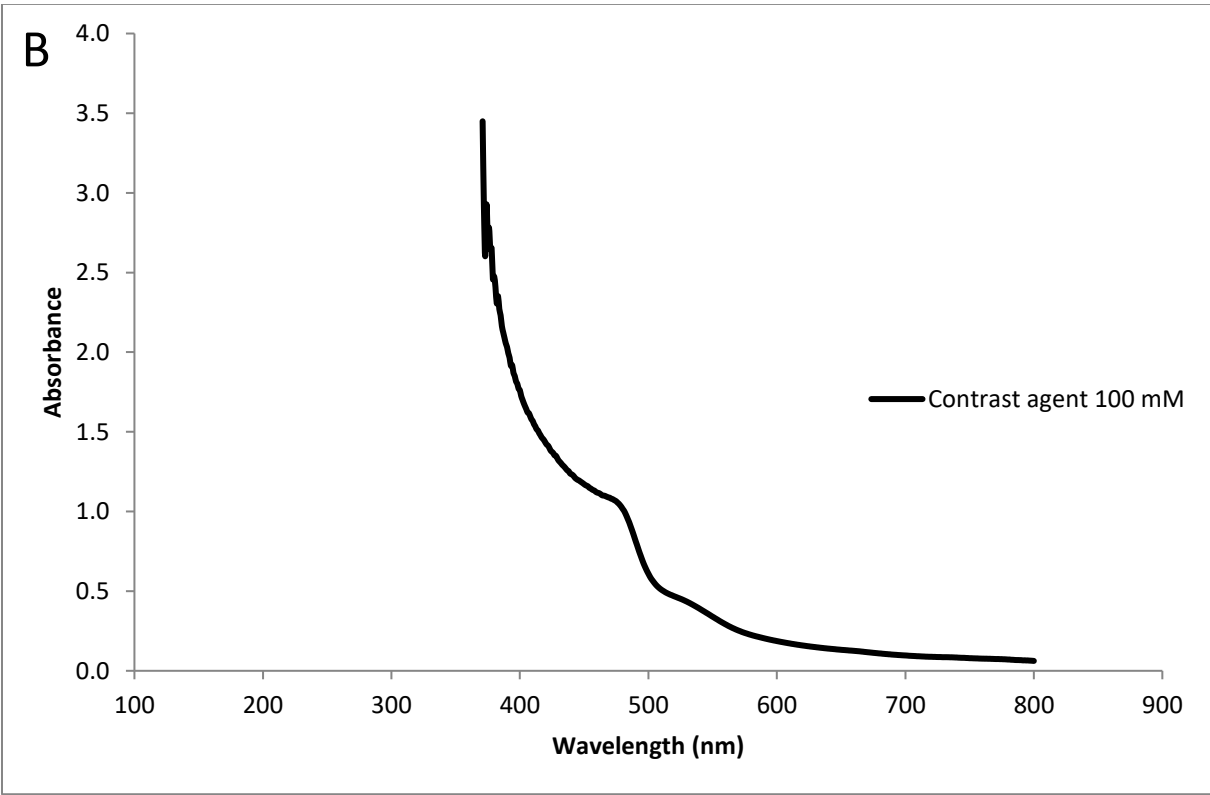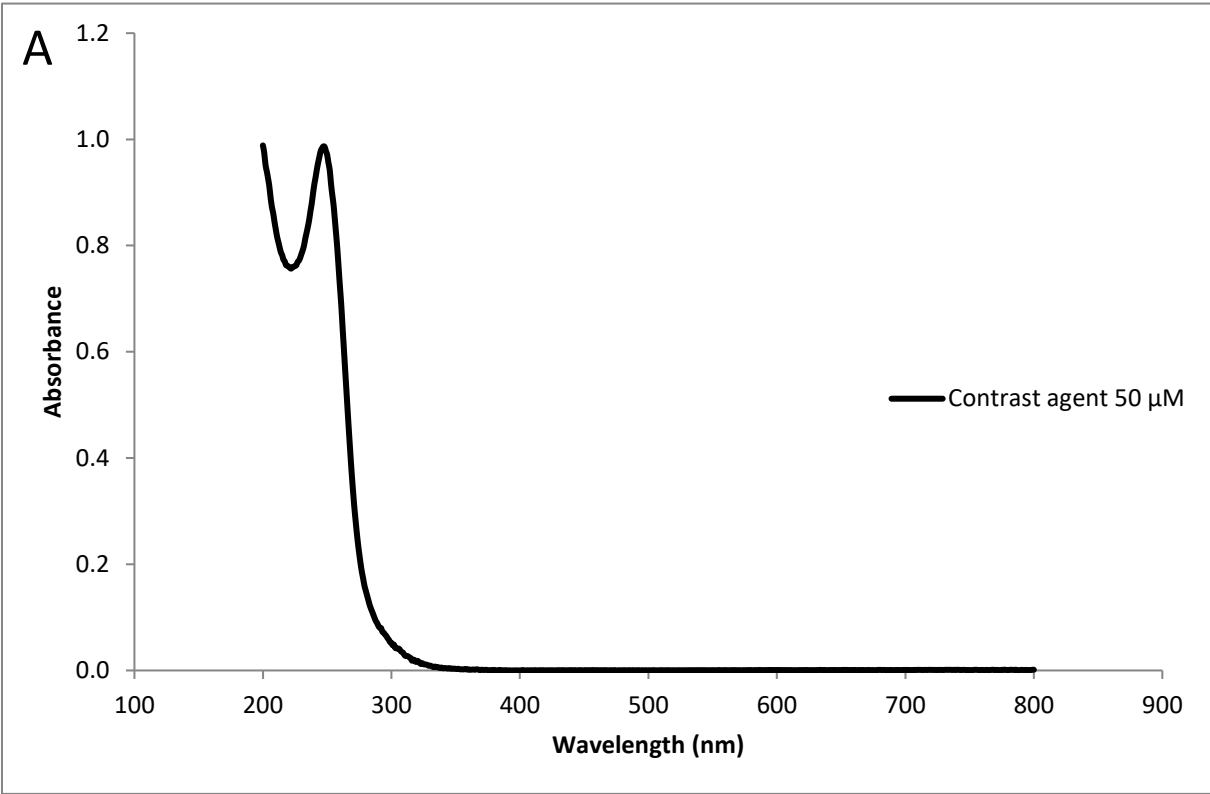
Supplemental Fig. S8: Absorption spectrum of the contrast agent. *A*: At a concentration of 50 µM, the contrast agent shows no absorption in the wavelengths used in fluorescence microscopy. *B*: At a concentration of 100 mM, there is absorption at those wavelengths due to the high concentration.

Supplemental Fig. S9: Fluorescent microscopy
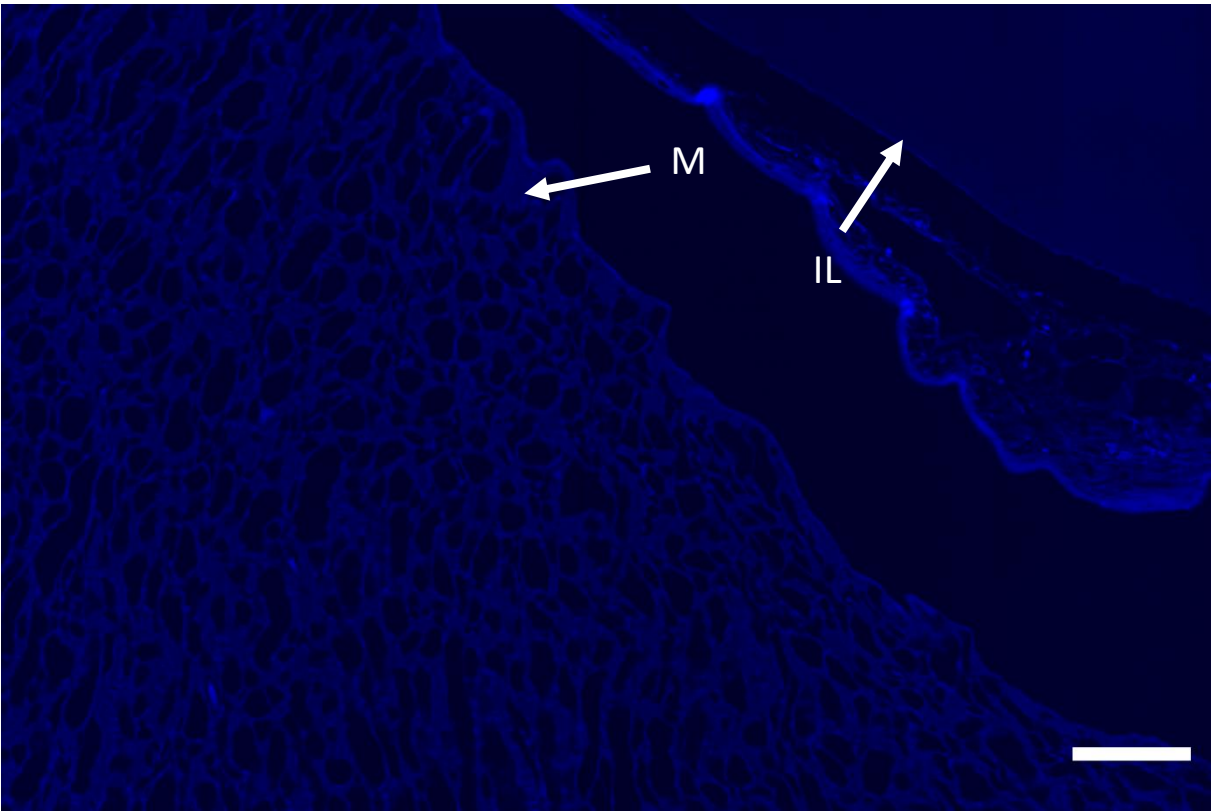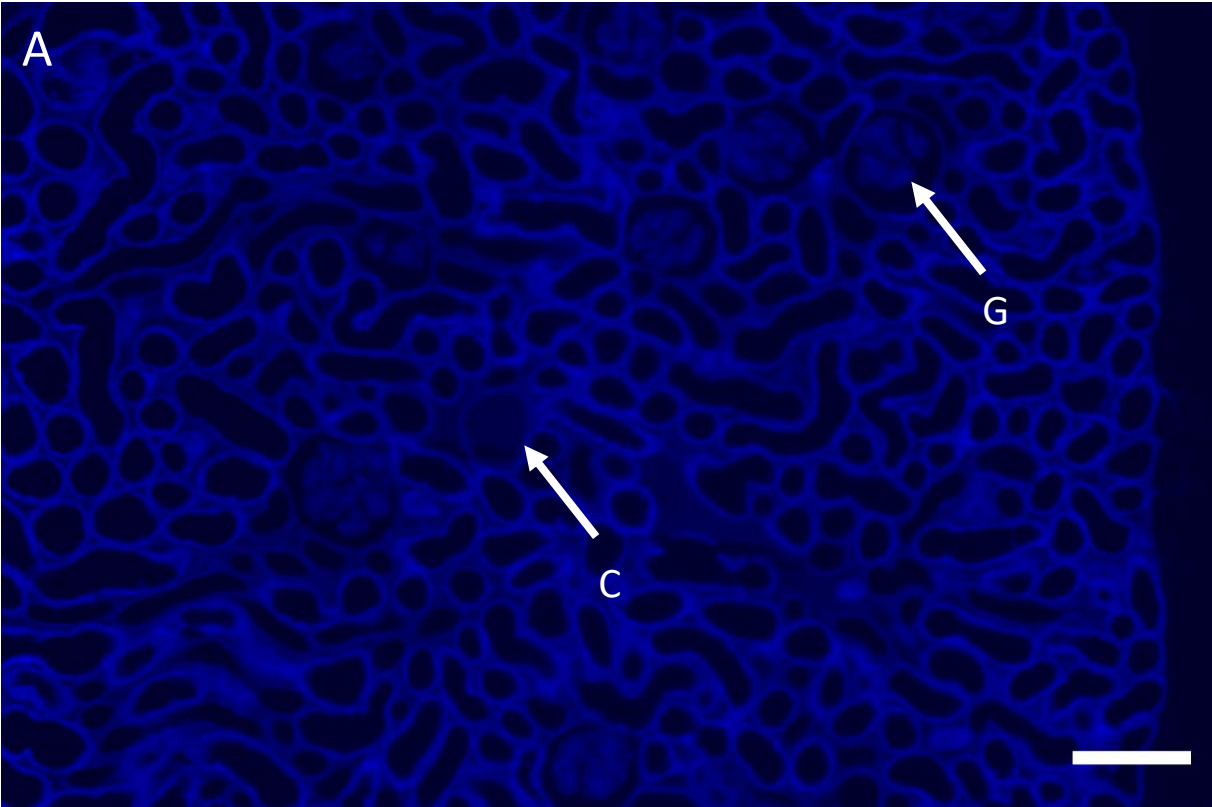
Supplemental Fig. S9: Fluorescent microscopy of the cortex and inner medulla in unstained kidney sections. Scale bars: 100 µm. *A*: DAPI channel, ex: 387 nm, em: 440 nm. X-ray contrast agent in glomerular tufts (G), cortical vessels (C) medullary capillaries (M) and an interlobar vessel (IL) shows less intense fluorescence compared to strong autofluorescence of the kidney.
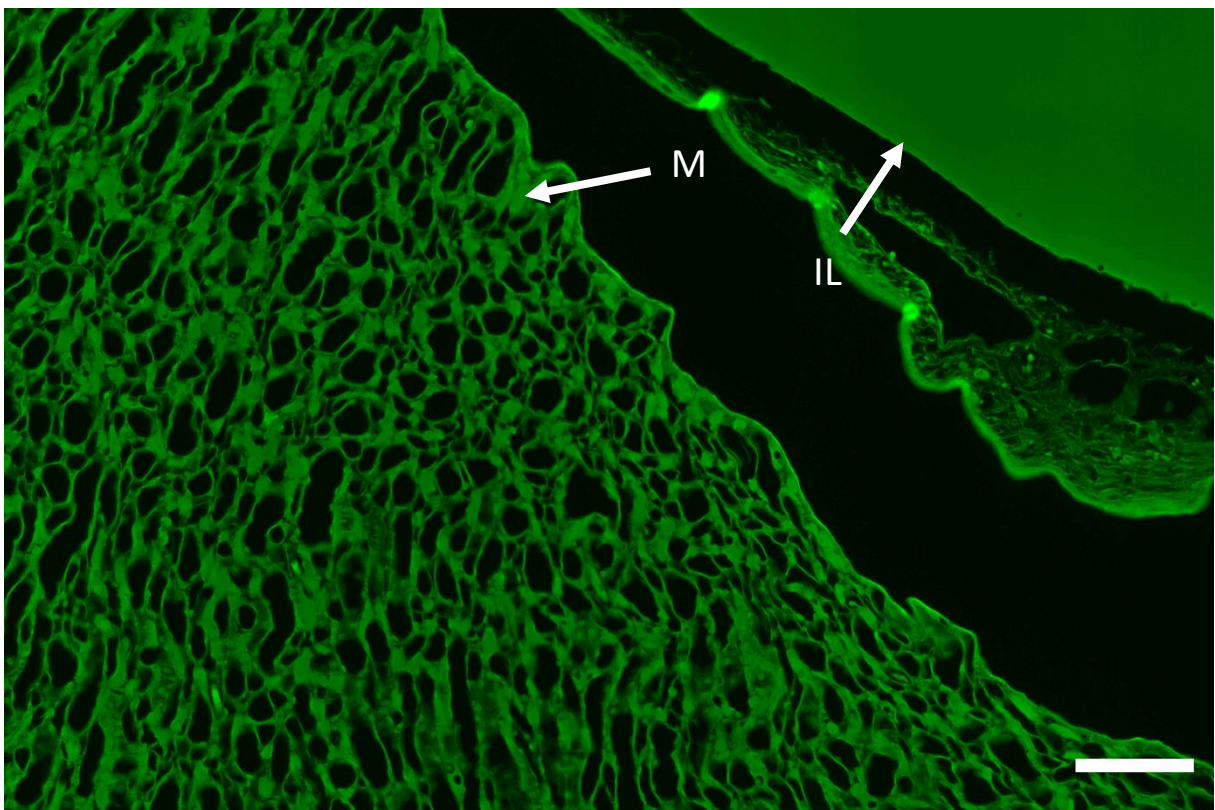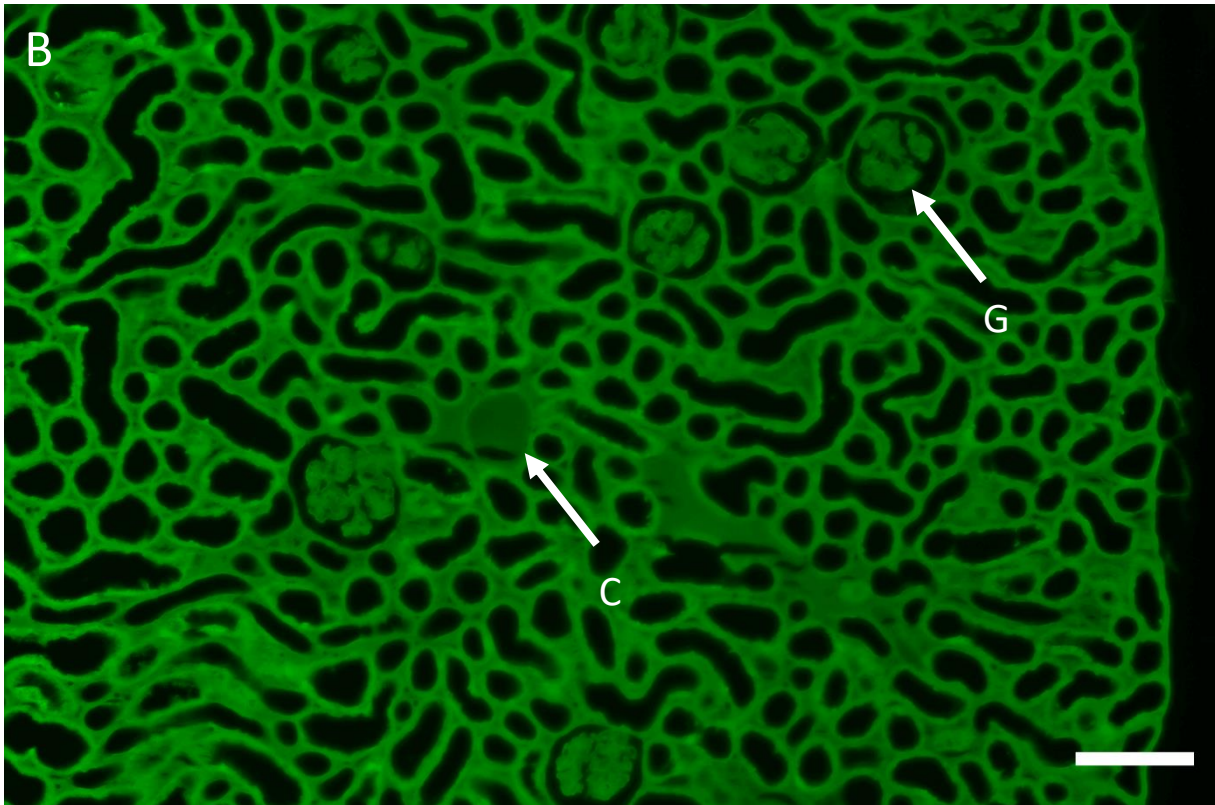
Supplemental Fig. S9: *B*: FITC channel, ex: 482 nm, em: 525 nm. X-ray contrast agent in glomerular tufts (G) and cortical capillaries (C) shows less intense fluorescence compared to strong autofluorescence of the kidney, while contrast agent capillaries in the inner medulla (M) shows comparable levels of fluorescence.
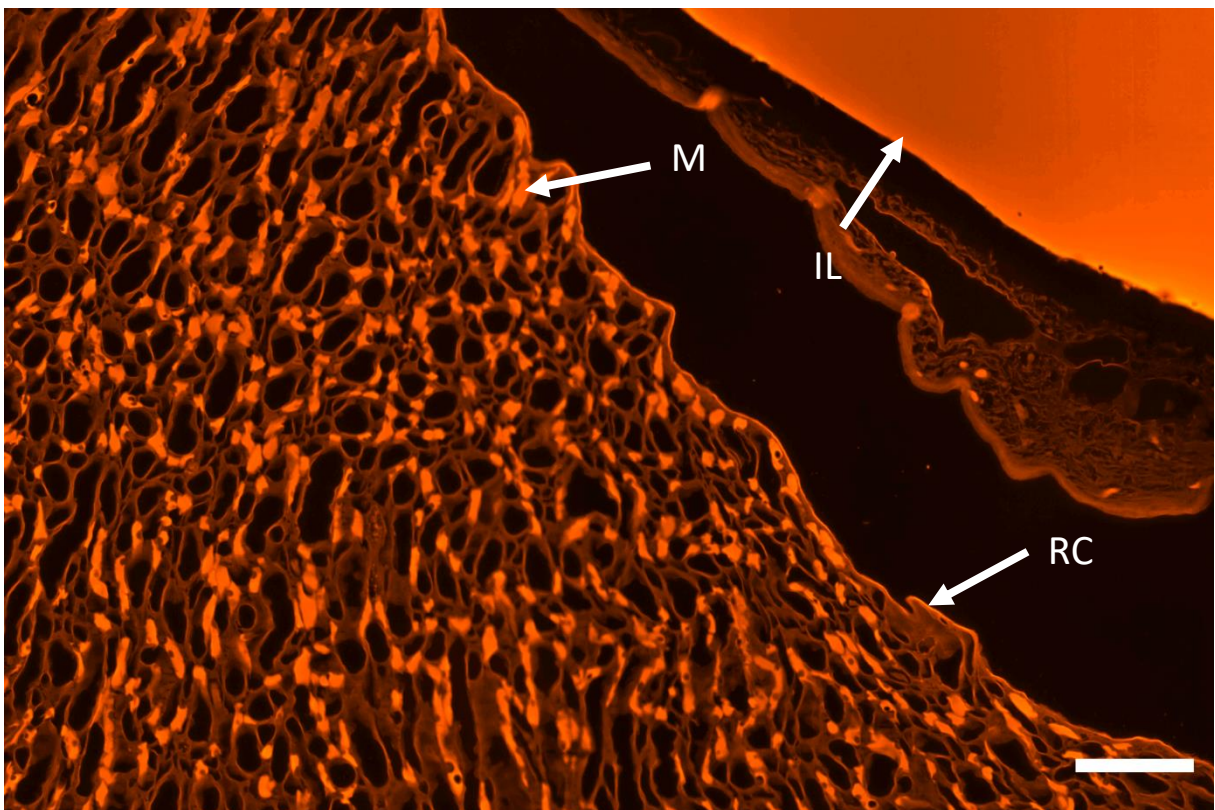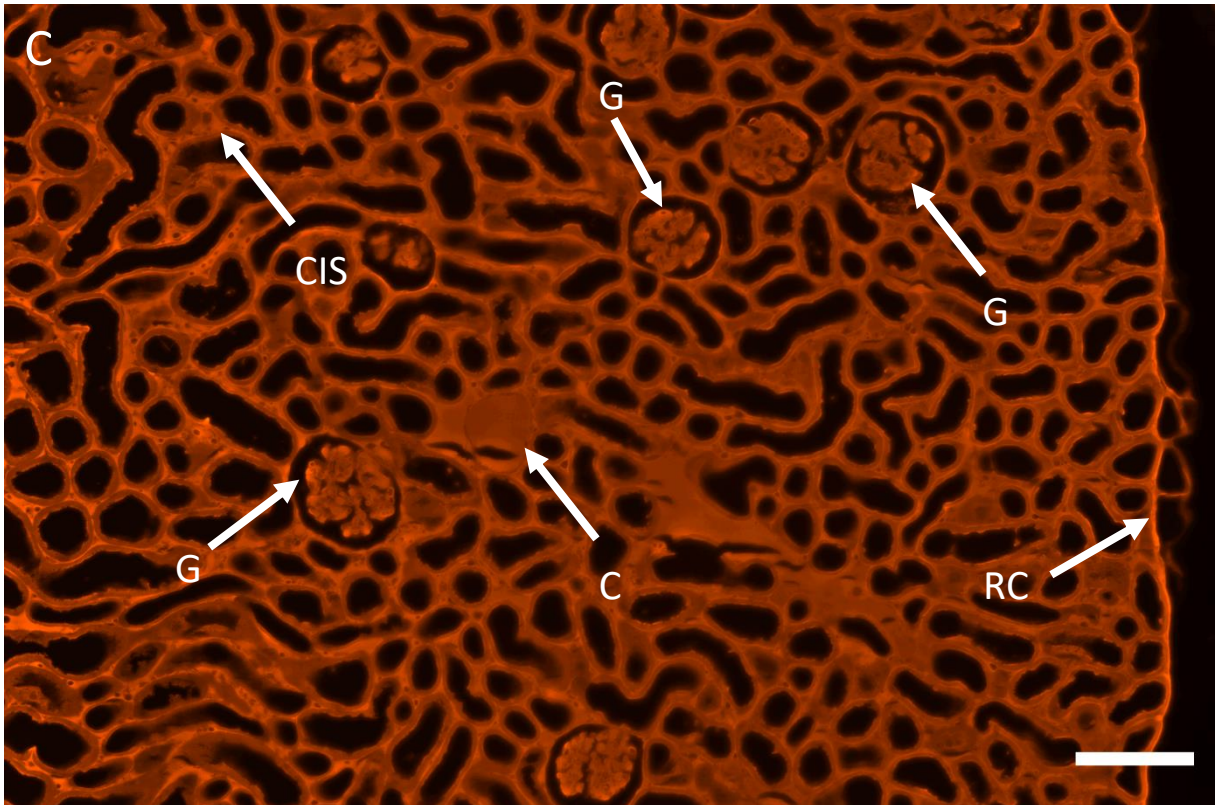
Supplemental Fig. S9: *C*: TRITC channel, ex: 563 nm, em: 607 nm. X-ray contrast agent shows much higher fluorescence than kidney autofluorescence in the interlobar vessel (IL) and capillaries of the inner medulla (M), and slightly elevated fluorescence in cortical vessels and glomerular tufts (G). Fluorescent signal can be seen in the cortical interstitium (CIS) and the renal capsule (RC), but these structures are not visible in X-ray µCT or electron microscopy, and are likely due to autofluorescence.

D
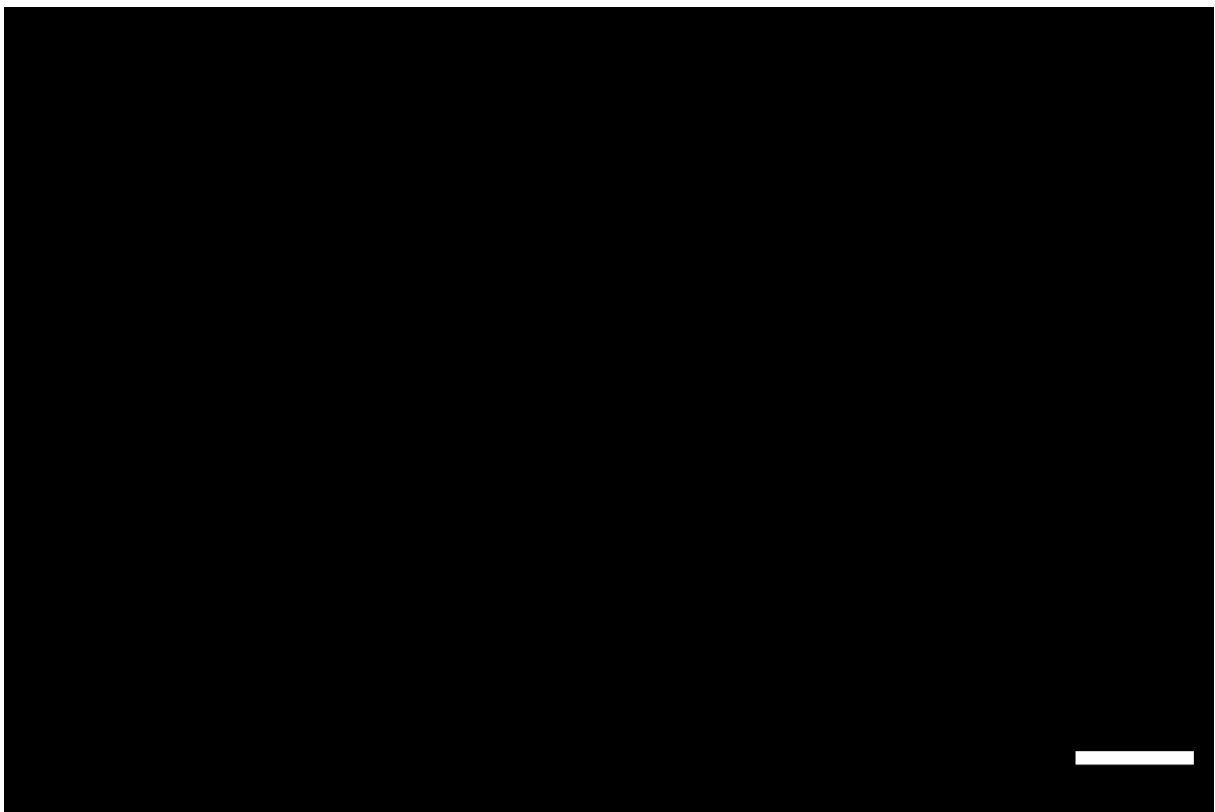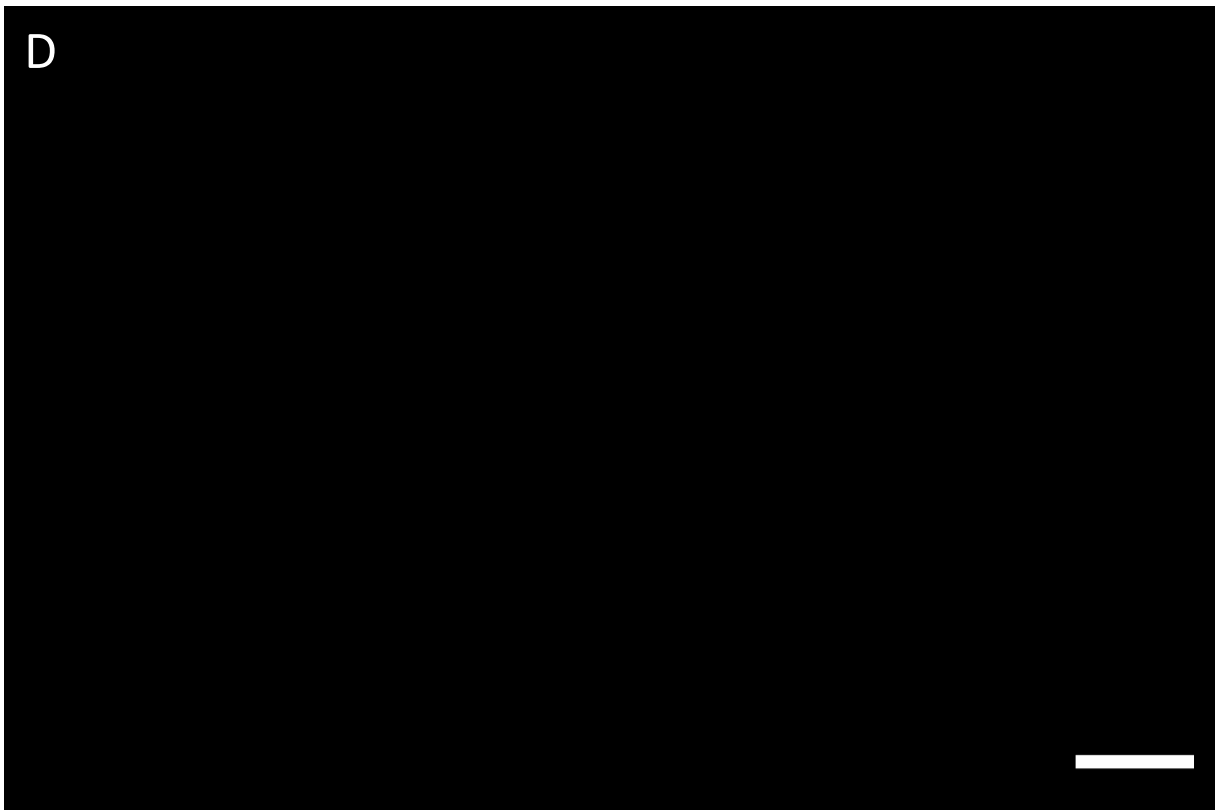
Supplemental Fig. S9: *D*: Cy5 channel, ex: 640 nm, em: 676 nm. No fluorescence of the contrast agent or autofluorescence of the kidney can be seen.

Detailed methods

Abdominal aorta perfusion

Kidneys were perfused retrogradely via the abdominal aorta based on a modified version of the isolated perfused kidney protocol by Czogalla et al. (Czogalla, et al., 2016).

A 50 ml syringe serving as reservoir was connected to a 2.5 m long silicone tube, and kept 2 m above the mouse for a hydrostatic pressure of 150 mmHg. A 3-way stopcock to control flow and a blunted butterfly needle were connected to the tubing with a Luer-lock connector. The whole tubing was then flushed thoroughly with water until all air bubbles had been removed. Perfusion solutions could later be added to the open reservoir on the top as needed, even under flow.

Mice were anaesthetized with ketamine/xylazine, using an initial dose of 100 mg/kg ketamine and 20 mg/kg xylazine. Additional doses of 25 mg/kg ketamine and 5 mg/kg xylazine were given in 15 min intervals if necessary. For each perfusion, three constrictor knot ligations had to be prepared: Two around the abdominal aorta, one above the renal artery and one below the renal artery, and one at the superior mesenteric artery. The constrictor knot was chosen, since the surgical knot does not hold sufficiently tight at pressures used in perfusion (Hazenfield & Smeak, 2014). Blood vessels were freed from surrounding fat, and silk sutures soaked in mineral oil were pulled under the vessel to be ligated using angled forceps. Abdominal aorta and vena cava had to be separated carefully from each other by pulling apart the fascia tubing holding them together without injuring either vessel.

The abdominal aorta was clamped above the lower abdominal aorta ligation. A small hole was cut into the abdominal aorta below the ligation, through which closed vessel dilating forceps could be inserted. The forceps were spread to insert a blunted 21 G butterfly needle between the tips deep enough to lie under the prepared ligation. The butterfly needle was first loosely fixed by pinning a pin behind one of the butterfly wings, then fixed properly to the abdominal aorta by tightening the prepared constrictor knot. The arterial clamp was removed, and the kidneys flushed with about 10 ml phosphate-buffered saline (PBS) and 100 ml 4% formaldehyde / 1% glutaraldehyde in PBS to fix the kidney under pressure and retain open tubular lumina. To prevent clogging of the capillaries, the aldehyde solution was pressed through a 1.2 µm syringe filter prior to perfusion. To quench leftover aldehydes prior to contrast agent perfusion, 20 ml PBS, 50 ml glycine solution (5 mg/ml in PBS) and another 40 ml PBS were perfused. All the above solutions were perfused at 37°C with 150 mmHg constant hydrostatic pressure.

Four ml of X-ray contrast agent solution (75 mg iodine/ml) were perfused using a 10 ml syringe, actuated with a 460 g weight to provide a constant pressure of around 150 mmHg. 4 ml are insufficient volume to build up the necessary hydrostatic pressure via the same silicon tubing as above.

Once contrast agent had been fully perfused, 4% glutaraldehyde in PBS was dripped into the abdominal cavity to start polymerization. Kidneys were cut out and kept in 4% glutaraldehyde in PBS. Care needs to be taken that renal artery and vein are cut cleanly in order to avoid accidentally pulling out the polymerized contrast agent hydrogel from the kidney vasculature.

For scanning, kidneys were mounted in 1% agar in PBS in 1.5 ml centrifugation tubes or 0.5 ml PCR tubes, depending on their diameter. Kidneys of mice with body weight below 25 g can typically fit into 0.5 ml PCR tubes.

Laboratory source X-ray microCT image acquisition

Laboratory source X-ray microCT images were acquired with a General Electric Phoenix Nanotom m system equipped with a water-cooled tungsten target and diamond window. Acceleration voltage was set to 60 kV, current 310 µA, no filter, Mode 0 for 2.2 – 2.7 µm focal spot size. The Nanotom m is equipped with a GE DXR Detector with 3072 × 2400 pixels, which was set to sensitivity setting 4, 0.5 s exposure time, 1440 projections per height step. The option to reduce ring artifacts through random detector position shift was turned on. Source detector distance was set to the minimum 225 mm, and sample was moved towards to a position close to the source to achieve 4.4 µm pixel size for standard 1.5 ml Eppendorf tubes and 3.3 µm pixel size for 0.5 ml PCR tubes. Directly before each scan, a 4-point calibration with 100, 170, 240, 310 µA was performed, with 50 flat-field frames recorded for each point and 50 dark-field frames recorded with the X-rays turned off.

For the 4.4 µm voxel size, 1.5 ml tube scans, 3 frames per projection were recorded and averaged per projection, resulting in a scan time of around 3.5 h per kidney.

For the 3.3 µm voxel size, 0.5 ml tube scan, 12 frames per projection were recorded and averaged per projection, resulting in a scan time of around 10 h per kidney.

Reconstruction was performed with the manufacturer's GE phoenix datos|x software. Projections were median filtered using a 3×3 kernel prior to reconstruction. Center of rotation calibration correction was optimized manually by reconstructing a single slice multiple times with different calibration values and selecting the best value via visual inspection. Images were cropped and exported as unsigned 16 bit values in a raw binary .vol file. Dimensions and other metadata were stored in the accompanying .pcr file.

Image processing – vascular and tubular segmentation of the 3.3 µm voxel size dataset

Segmentation of the 3.3 µm voxel size X-ray data was performed using Fiji/ImageJ (Schindelin, et al., 2012; Schneider, et al., 2012) with the MorphoLibJ (Legland, et al., 2016) and 3D ImageJ Suite plugins (Ollion, et al., 2013). These can be installed by adding the following update sites: http://sites.imagej.net/IJPB-plugins/ and http://sites.imagej.net/Tboudier/ .

The kidney dataset was imported via raw import and cropped again, reducing the data size from 46 GB to 21 GB. The whole volume was filtered with the Fiji 3D Gauss filter function, using an isotropic σ = 1 voxel. Blood vessels and tubules were extracted by setting manual thresholds. As the first height step of the scan had a deviating intensity distribution from the other height steps, thresholds were set separately from the rest of the scan.

For blood vessels, a lower threshold of 27700 was chosen for the first height step, and a lower threshold of 27000 for the rest of the dataset. To remove contrast from contrast agent stuck to the outside of the kidneys, a mask was created by choosing another threshold of 23000 for the whole kidney, performing MorphoLibJ's 6-connected component labeling function to label and remove unconnected areas via thresholding. As the first mask still left some areas connected to the kidney, a single 3D erosion was performed and the connected component labeling repeated. The mask was 3D dilated two times and applied to the blood vessel segmentation, yielding the blood vessel segment.

For tubules, upper thresholds of 25000 and 24200 were chosen, respectively. To separate tubules from the water background with the same intensity, a kidney shape mask was created from the blood vessel segment by dilating at first 10 times and using 3D ImageJ Suite 3D hole filling. As there were still holes remaining, we dilated the mask another 3 times, repeated the 3D hole filling, then eroded the

shape back 13 times. The resulting kidney shape mask was applied to the thresholds to receive the tubule segment.

Quantification of vessel and tubular volumes and surface was performed with Analyze Regions 3D of the MorphoLibJ plugin. The plugin calculated the volume based on the number of voxels in the binary segment, and surface was estimated by counting the number of line probe intersections in 13 different directions. Details can be found in the MorphoLibJ documentation: https://imagej.net/MorphoLibJ

We manually chose a marker point at the papilla of the kidney in the blood vessel segment at X: 370, Y: 1671, Z: 1194 and calculated the lengths of the shortest path along the blood vessels using the Geodesic Distance Map 3D function of MorphoLibJ. The Euclidean distance map and all histograms were calculated using default Fiji/ImageJ functions.

All image processing was performed on a workstation equipped with 256 GB RAM and two eight-core Intel Xeon E5-2670 processors clocked at 2.60 GHz. 3D computer graphic images of the segmentation were rendered with Arivis4D 2.12.4 (Arivis, Germany) on a virtual machine with 174 GB of RAM, 7 Intel Xeon E5-2680 v2 cores and pass-through Nvidia Grid K2 graphics.

Materials and Suppliers List

Perfusion reagents

Phosphate Buffered Saline (PBS)	Oxoid Phosphate Buffered Saline Tablets (Dulbecco A) BR0014G , ThermoFisher Scientific, United States
Ketamine 100 mg/ml	Ketasol®-100 ad us. vet., Injektionslösung Dr. E. Graeub AG, Switzerland
Xylazine 20 mg/ml	Xylazin Streuli ad us. vet., Injektionslösung Streuli Pharma AG, Switzerland
Paraformaldehyde	Paraformaldehyde prilled, 95% 441244, Sigma Aldrich, Germany
Glycine	Glycine Molecular biology 07132391, Biosolve Chimie, France
Agar	Agar for microbiology 05039, Sigma Aldrich, Germany
Mineral oil	Mineral oil, light oil (neat), BioReagent M8410, Sigma Aldrich, Germany

Surgical Tools

Fine scissors	Vannas Spring Scissors - 2.5mm Blades 15000-08, Fine Science Tools, Germany
Arterial clamp	Micro Serrefine - 10 x 2 mm 18055-01, Fine Science Tools, Germany
Arterial clamp applying forceps	Micro-Serrefine Clip Applying Forceps 18057-14, Fine Science Tools, Germany
Vessel dilating forceps	S&T Vessel Dilating Forceps - 11cm 00125-11, Fine Science Tools, Germany
Angled forceps	S&T 0.3mm x 0.25mm Forceps 00649-11, Fine Science Tools, Germany
Straight forceps	Rubis Switzerland Tweezers 5-SA 232-1221, VWR, United States
Silk suture for ligations	Non-Sterile Silk Suture Thread 5/0 18020-50, Fine Science Tools, Germany

Perfusion Consumables

1 ml syringe	Injekt F 1 ml 9166017V , B. Braun, Germany
26 G needle	Sterican 26 G x ½ " 466 5457, B. Braun, Germany
10 ml syringe Luer Lock	NORM-JECT 10 ml (12 ml) 4100-X00V0, Henke Sass Wolf, Germany
50 ml syringe Luer Lock	Omnifix 50 ml (60 ml) 4617509F , B. Braun, Germany
1.2 µm syringe filter	Chromafil Xtra PET-120/25 729229, Macherey-Nagel, Germany
3-way stopcock	Discofix C 3-way Stopcock 16494C , B. Braun, Germany
21 G butterfly needle	Venofix Safety G21 4056521-01, B. Braun, Germany
0.5 ml PCR tubes	PCR Single tubes, PP, 0,5 ml 781310, Brand, Germany
1.5 ml centrifugation tubes	Micro tube 1.5ml 72.690.001, Sarstedt, Germany

References

CZOGALLA, J., SCHWEDA, F. & LOFFING, J. (2016). The Mouse Isolated Perfused Kidney Technique. J Vis Exp (117), 54712.

HAZENFIELD, K.M. & SMEAK, D.D. (2014). In vitro holding security of six friction knots used as a first throw in the creation of a vascular ligation. J Am Vet Med Assoc **245**(5), 571-577.

LEGLAND, D., ARGANDA-CARRERAS, I. & ANDREY, P. (2016). MorphoLibJ: integrated library and plugins for mathematical morphology with ImageJ. Bioinformatics **32**(22), 3532-3534.

OLLION, J., COCHENNEC, J., LOLL, F., ESCUDE, C. & BOUDIER, T. (2013). TANGO: a generic tool for high-throughput 3D image analysis for studying nuclear organization. Bioinformatics **29**(14), 1840-1841.

SCHINDELIN, J., ARGANDA-CARRERAS, I., FRISE, E., KAYNIG, V., LONGAIR, M., PIETZSCH, T., PREIBISCH, S., RUEDEN, C., SAALFELD, S., SCHMID, B., TINEVEZ, J.Y., WHITE, D.J., HARTENSTEIN, V., ELICEIRI, K., TOMANCAK, P. & CARDONA, A. (2012). Fiji: an open-source platform for biological-image analysis. Nat Methods **9**(7), 676-682.

SCHNEIDER, C.A., RASBAND, W.S. & ELICEIRI, K.W. (2012). NIH Image to ImageJ: 25 years of image analysis. Nat Methods **9**(7), 671-675.